

AD-A111 785

CLEMONSON UNIV SC DERTY OF MECHANICAL ENGINEERING

F/S 20/4

ROTATIONAL FLOW IN A CURVED-WALL DIFFUSER DESIGNED BY USING THE--ETC(U)

MAY 81 T YANG, F NTONE

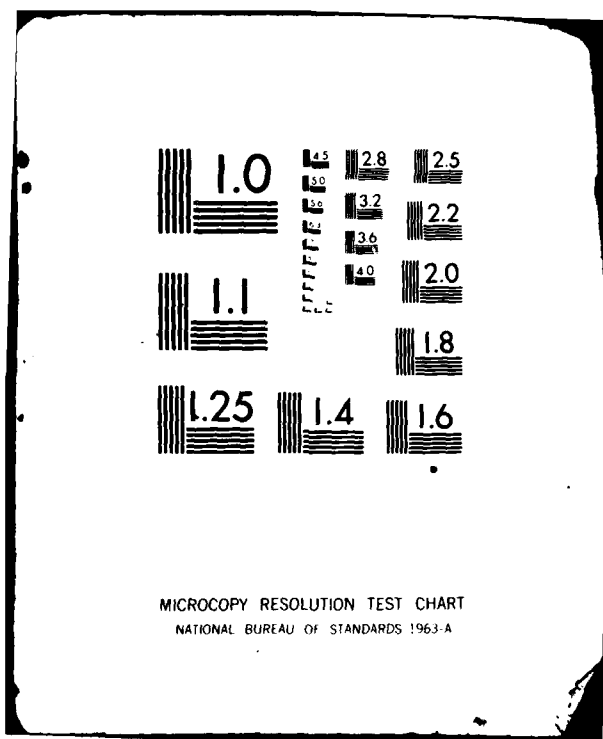
UNCLASSIFIED

ML

1-1  
2-1



END  
DATE  
FILMED  
4-82  
DTIC



23

ADA111785

ROTATIONAL FLOW IN A CURVED-WALL DIFFUSER DESIGNED BY USING THE INVERSE  
METHOD OF SOLUTION OF POTENTIAL FLOW THEORY

Tah-teh Yang and Francois Ntone  
Mechanical Engineering Department, Clemson University  
Clemson, South Carolina

14 MAY 81

ABSTRACT

Curved wall diffusers designed by using an inverse method of solution of potential flow theory have been shown to be both short and highly efficient. These features make this type of diffuser attractive in thrust ejector applications. In ejectors, however, the flow at the diffuser inlet is nearly a uniform shear flow. This paper presents a method used in examining the flow velocity along the diffuser wall and some of the analytical results for diffusers designed with potential flow theory and receiving a rotational flow. The inlet flow vorticity and the diffuser area ratios prescribed in the inverse solution of the irrotational flow are the parameters of the study. The geometry of a sample ejector using such a diffuser and its estimated thrust augmentation ratio are also presented.

INTRODUCTION

The existing "Clemson Inverse Design Program for Short Curved Wall Diffusers"<sup>1</sup> is based on irrotational flow theory. Much experimental data have been examined for inlet flows having thin boundary layers with core flows well represented by potential flow theory. In such cases, experimentally obtained wall pressure distributions agree with the theoretically prescribed distributions very well. In ejectors, however, the diffuser inlet flow is significantly different from irrotational flow.

Based on the inlet velocity measurements reported by Hill and Gilbert<sup>2</sup> it appears that diffuser inlet flow should be represented by a shear flow of uniform vorticity. Under this condition (admitting a shear flow) the wall pressure distribution could be significantly different from that which was prescribed for the particular diffuser inlet design. Specifically, this raises a concern about the presence of an adverse pressure gradient or a deceleration in diffuser wall velocity which may result from the inlet shear flow. A moderate deceleration upstream of the suction slot may be overcome by increasing the suction flow rate. A strong deceleration will result in flow separation. A combination of large design area ratio and inlet vorticity could also result in a flow reversal at the diffuser exit because of the shear flow requirement, even in an inviscid flow. It becomes apparent, therefore that a method of calculating the wall velocity of a shear flow in this type curved diffuser is necessary to assure no adverse pressure gradient along the diffuser wall. And this will allow us to obtain the high thrust augmentation benefit afforded by using a short, curved wall diffuser section in the ejector design.

WDC FILE COPY

## METHOD OF SOLUTION

### 1. Equations of Motion

The coordinate system is defined by Figure 1. For axisymmetric flow, the continuity equation is:

$$\frac{\partial u}{\partial r} + \frac{\partial w}{\partial x} + \frac{u}{r} = 0 \quad (1)$$

Define the stream function  $\Psi(r, x)$  such that:

$$w = \frac{1}{r} \frac{\partial \Psi}{\partial r} \quad \text{and} \quad u = -\frac{1}{r} \frac{\partial \Psi}{\partial x} \quad (2a, b)$$

Then equation (1) becomes:

$$\frac{1}{r^2} \frac{\partial \Psi}{\partial x} - \frac{1}{r} \frac{\partial^2 \Psi}{\partial r \partial x} + \frac{1}{r} \frac{\partial^2 \Psi}{\partial x \partial r} - \frac{1}{r} \left( \frac{1}{r} \frac{\partial \Psi}{\partial x} \right) = 0$$

In addition,  $\Psi$  satisfies the vorticity equation which in cylindrical coordinates for an axisymmetric shear flow is:

$$\frac{\partial u}{\partial x} - \frac{\partial w}{\partial r} = B \quad (3)$$

Substituting equations (2a, b) into equation (3) yields the following

$$\frac{\partial^2 \Psi}{\partial x^2} + \frac{\partial^2 \Psi}{\partial r^2} = \frac{1}{r} \frac{\partial \Psi}{\partial r} - Br \quad (4)$$

which is an elliptic partial differential equation.

### 2. Boundary Conditions

In the numerical solution of equation (4), for shear flow, we used the same grid network as for irrotational flow. The boundary conditions used are as follows.

#### (1) Inlet

At the diffuser inlet, there is a parallel flow in the x-direction, and consequently  $u = 0$ . The  $\Psi$ 's are obtained from equations (2a, b) as follows

$$\frac{1}{r} \frac{\partial \Psi}{\partial r} = w \quad \text{and} \quad -\frac{1}{r} \frac{\partial \Psi}{\partial x} = 0$$

Therefore  $\Psi$  only changes with  $r$ , hence

$$\frac{d\Psi}{dr} = wr$$

For shear flow,

$$w = w_{0, \text{in}} - Br$$

therefore

$$\Psi = \int_0^r r(w_{0, \text{in}} - Br) dr$$

Which yields

$$\psi = \frac{1}{2} r^2 w_{o,in} - \frac{1}{3} Br^3 \quad (5)$$

From equation (5), we have:

$$\psi_{wall} = \frac{1}{2} R_{in}^2 w_{o,in} - \frac{1}{3} BR_{in}^3 \quad (6)$$

where  $R = r(\psi_{wall})$

For irrotational flow and uniform parallel inlet velocity  $q_{irr}$ , we have:

$$\psi_{irr} = \int_0^{R_{in}} r q_{irr} dr$$

At the wall:

$$(\psi_{irr})_{wall} = \frac{1}{2} q_{irr} R_{in}^2 \quad (7)$$

However,  $\psi_{wall}$  may not necessarily be equal to  $(\psi_{irr})_{wall}$ , which means that for the same diffuser geometry, flow rates for the irrotational and rotational (shear) cases may not be the same.

Define  $\gamma$  such that

$$(\psi_{irr})_{wall} = \gamma \psi_{wall}$$

and then

$$q_{irr} = \gamma(w_{o,in} - \frac{2}{3} BR_{in}) \quad (8)$$

For the shear flow solution, we will need to (i) specify, for the inlet boundary condition, the values of  $w_{o,in}$  and  $\gamma$ ; (ii) obtain  $B$  from equation (8); and (iii) specify the streamline according to equation (5).

Another possibility is that both  $B$  and  $w_{o,in}$  are specified, and  $\gamma$  is to be calculated from equation (8).

In the inverse design program if we have prescribed parallel but non-uniform irrotational flows at the inlet and the exit, then the boundary condition at the inlet would be as follows:

$$(\psi_{irr})_{wall} = \gamma \left[ \frac{1}{2} R_{in}^2 w_{o,in} - \frac{1}{3} BR_{in}^3 \right]$$



Accession For	<input checked="" type="checkbox"/> <input type="checkbox"/> <input type="checkbox"/>
NTIS GRA&I	
DTIC TAB	
Unannounced	
Justification	
By	
Distribution	
Availability	

A

For known B and  $w_{o,in}$ ,  $\gamma$  can be calculated from the following

$$\gamma = \frac{(\psi_{irr})_{wall}}{\frac{1}{2} R_{in}^2 w_{o,in} - \frac{1}{3} B R_{in}^3} \quad (9)$$

and the streamlines can be calculated from equation (5).

(2) Centerline

Along the centerline, we have  $\psi = 0$ .

(3) Wall, upstream of slot

Along the wall, upstream of the slot, we have  $\psi = \psi_{wall}$ , where  $\psi_{wall}$  is the same as the one calculated at the inlet.

(4) Wall, downstream of slot and inside of slot

Let  $\beta$  and  $\beta_{irr}$  be the fractions of the flow into the slot for the rotational and irrotational cases respectively. These  $\beta$ 's are related to the stream functions as shown in the following expressions.

$$\beta_{irr} = 1 - \frac{\psi_{irr,st}}{\psi_{irr,wall}} \quad (10)$$

and

$$\beta = \frac{\psi_{wall} - \psi_{st}}{\psi_{wall}}$$

or

$$\psi_{st} = \psi_{wall} (1 - \beta) \quad (11)$$

$\beta$  is specified as an input to the analysis. The  $\psi$  values for lines AB and AC in Figure 2 are determined from equation (10).

(5) Diffuser Exit

Letting  $Q_{irr}$  = Volumetric flow rate at the diffuser exit for irrotational flow and

$Q$  = Volumetric flow rate at diffuser exit for shear flow

results in:

$$Q_{irr}/(1 - \beta_{irr}) = \gamma Q/(1 - \beta) \quad (12)$$

It can be shown that for parallel flow

$$w_{o,e} = \frac{2}{3} B R_{NSTAGU} + \frac{2(\psi_{irr})_{wall}(1 - \beta)}{\gamma R_{NSTAGU}^2} \quad (13)$$

Here  $B$  is specified,  $\psi_{irr}$  and  $R_{NSTAGU}$  are obtained from the Clemson Inverse Solution Computer Program, and  $w_{o,e}$  is the center line velocity at the diffuser exit. ( $R_{NSTAGU}$  is the radius at the stagnation point A of Figure 2.)

#### (6) Exit of Slot

At the slot exit, a shear flow having vorticity  $B$  is assumed.

Referring to Figure 4:

$$R - R_o = y \sin(90^\circ - \alpha) = y \cos \alpha$$

or

$$R = R_o + y \cos \alpha \quad (14)$$

The following development is to determine the stream function in the slot.

$$\psi_y - \psi_{st} = \int_0^y q R dy \quad (15)$$

But from Figure 3 we see that,  $q = q_{o,sl} - By$

and therefore

$$\psi_y = \psi_{st} + R_o q_{o,sl} y + \frac{1}{2} (q_{o,sl} \cos \alpha - R_o B) y^2 - \frac{1}{3} B y^3 \cos \alpha \quad (16)$$

The  $\psi$ 's at the exit of the slot can be prescribed using equation (15) where  $y$  is replaced by  $\frac{(R-R_o)}{\cos \alpha}$ , viz.

$$q_{o,sl} = \frac{\beta \psi_{wall} + \frac{1}{2} R_o B \frac{R_{w,sl} - R_o}{\cos \alpha} + \frac{1}{3} B \frac{R_{w,sl} - R_o}{\cos \alpha} \cos \alpha}{R_o \frac{R_{w,sl} - R_o}{\cos \alpha} + \frac{1}{2} \frac{R_{w,sl} - R_o}{\cos \alpha} \cos \alpha} \quad (17)$$

### 3. Computational Procedures

- (1) For irrotational flow, prescribe  $q_{irr}$  parallel at inlet and exit of diffuser. Prescribe a slightly increasing velocity distribution at wall, upstream and downstream of the slot, with desired deceleration across the slot region.
- (2) Solve the inverse problem for irrotational flow. The grid work in terms of  $x$ 's and  $r$ 's and the velocity distributions at inlet and exit of the diffuser and at the slot exit are then obtained.
- (3) Solve the rotational flow equation for  $\psi$  using the previously discussed boundary conditions.
- (4) Solve for the velocity distribution at the wall. If the velocity distribution at the wall is slightly increasing with an abrupt deceleration across the slot, the diffuser geometry is satisfactory. If there is a deceleration along the wall, change the irrotational wall velocity distribution and go back to (2).

Using equations (2a,b) we may compute the velocity distribution along the wall from the  $\Psi$  distribution, i.e., with

$$q = \sqrt{\left(\frac{1}{r} \frac{\partial \Psi}{\partial r}\right)^2 + \left(\frac{1}{r} \frac{\partial \Psi}{\partial x}\right)^2} \quad (18)$$

In the wall velocity computation, the vorticity is to be specified as one of the parameters at the diffuser inlet, and in ejector application this parameter is determined from the mass ratio of the primary and the secondary flow rates and the geometry of the mixing chamber. Using this method, computations were carried out on the University's IBM 370/3033 digital computer. Before a more generalized inverse design program is formulated, the method outlined above will be used to examine the wall velocity distribution to assure the absence of any adverse pressure gradient in ejector design. A more detailed version of the analysis will be published as Mr. Francois Ntone's thesis for a Master of Science Degree in Mechanical Engineering at Clemson University, which is expected to be completed by May 1981. Results of the sample computations using the above outlined analysis are presented in the next section.

#### ANALYTICAL RESULTS

Figure 5 represents an axisymmetric diffuser having an area ratio of 2.5 to 1. Figure 6 shows the velocity distributions along the diffuser walls. The circles denote the velocity distribution prescribed to the "Inverse Design Program" for irrotational flow, and the triangles represent the velocity distribution along the diffusers depicted in Figure 5. The second velocity distributions were computed for inlet shear flow having a nondimensional vorticity value of 0.33 where velocity and length are normalized by inlet center line velocity and inlet width respectively. It is apparent that even though the prescribed diffuser wall velocity distribution upstream of the slot has a strong acceleration, the wall velocity distributions may experience deceleration in the diffuser when a shear flow is admitted. In actual operation a flow separation would most likely take place.

Figure 7 shows three velocity distributions for the diffuser depicted in Figure 5; these are specifically for inlet vorticity values of 0.33, 0.5, and 0.65. There is a significant change in the magnitude of the velocities, but their gradients vary only slightly. As expected, larger vorticity results in more deceleration. The larger change of wall velocity magnitude results from the assumption in our analysis that the diffuser center line velocity is kept constant, therefore the wall velocity decreases more when the inlet shear flow vorticity increases more. Judging from the distributions of this figure, a flow separation would likely take place in all three cases. Figure 8 shows the wall velocity distributions for the diffuser depicted in Figure 5, under the conditions of (i) admitting an inlet shear flow with a vorticity of 0.5 and (ii) three different slot suction rates. A suction rate of 5.6% was the design value. At a suction rate of 8.5%, the velocity gradient upstream of the slot has not improved significantly in comparison to the distribution resulting from the 5.6% suction flow. Perhaps none of these distributions will yield a fully attached flow throughout the diffuser.



Figure 9 shows a diffuser designed for irrotational flow and having an area ratio of 2.5 to 1 with its suction slot slightly modified. Figure 10 shows the rotational velocity distribution along the walls of diffusers depicted in Figures 1 and 5 with inlet vorticity of 0.5. Apparently, there is no significant difference in wall velocity distribution for these two shear flow inlet cases. Figure 11 shows a diffuser designed for irrotational flow and having an area ratio of 2 to 1. Figure 12 shows wall velocity distributions for the diffuser depicted in Figure 11. The velocity distribution represented by circles is for irrotational flow, and that represented by triangles is for shear flow with velocity of 0.5. In this case hardly any deceleration is detected for the rotational flow, therefore, one should expect a highly effective diffuser even when a shear flow inlet condition is imposed at the curved wall diffuser inlet. Figures 13 and 14 are similar to Figure 12 and are for an area ratio of 1.5 to 1.

#### SAMPLE EJECTOR

Now the variation of wall velocity distribution due to vorticity is understood, and one may select ejector design parameters in such a way that no deceleration takes place along the diffuser wall and the diffuser flow can be maintained attached without excessive boundary layer suction.

Figure 15 shows an example of an air-to-air ejector for thrust augmentation with the area ratio of the secondary flow to the primary flow at the mixing chamber inlet of 40 to 1, and the mass ratio of the secondary flow to primary flow of 12 to 1. This ejector has a static pressure of  $-1.25/\text{psig}$  at the exit of a mixing chamber. From this pressure level one may use a highly effective short diffuser with an area ratio of 2.2 to achieve an exit pressure of the ambient level.

Based on the conventional definition of thrust augmentation ratio  $\phi$ , namely; the momentum of the mixture of the primary and secondary flows at the ejector exit to the momentum of the primary flow at the mixing chamber inlet, this sample ejector has a value of  $\phi$  of 2.182. Since the short diffuser of the sample ejector uses boundary layer control, an auxiliary ejector will be used to achieve the necessary boundary layer suction. The removed air will be discharged in the same direction as the thrust ejector and thus contributes to the overall thrust. Therefore a modified thrust augmentation ratio  $\phi_2$ , defined as the total momentum at the ejector exit to the sum of the momentum of the primary flows at the mixing chamber inlet and the suction chamber, must be used for this type of ejector. We found that for the sample ejector,  $\phi_2$  has a value of 1.830 provided that a suction fraction of 10% is adequate for the boundary layer control, and the mass ratio of the auxiliary ejector of 4 to 1 can be accomplished. These assumptions are considered to be reasonable. It is noteworthy that the overall length of the ejector is much reduced relative to the ones having diffusers designed by using the concept of incipient separation. The performance level in thrust augmentation ratio compared favorably to those reported in reference 3.

#### REFERENCES

1. Nelson, C.D. and T. Yang, "Design of Bounded and Unbounded Axially Symmetrical Ducts with Specified Distributions", AIAA Journal, Vol. 15, No. 9, Sept. 1977.
2. Gilbert, G.B. and P.G. Hill, "Analysis and Testing of Two-Dimensional Slot Nozzle Ejectors with Variable Area Mixing Sections", NASA CR 2251, Nov. 1972.
3. Tai, T.C., "Optimization of Axisymmetric Thrust Augmenting Ejectors", Proceedings of AIAA 10th Fluid and Plasmadynamics Conference, Albuquerque, New Mexico, June 27-29 1977, paper 77-707.

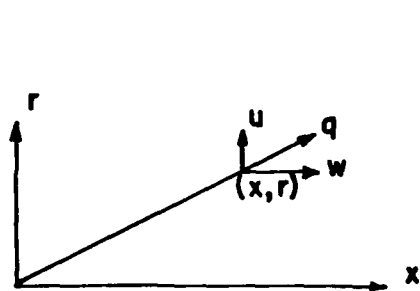


Figure 1. Coordinate System and Velocity Components

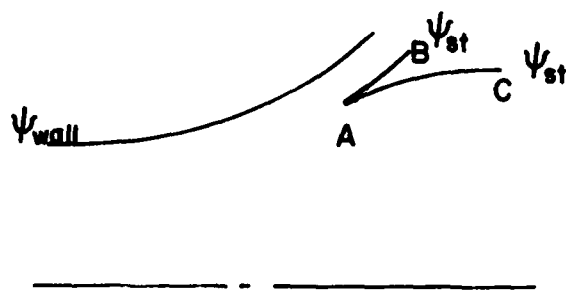


Figure 2. Wall Streamlines and the Branching Point

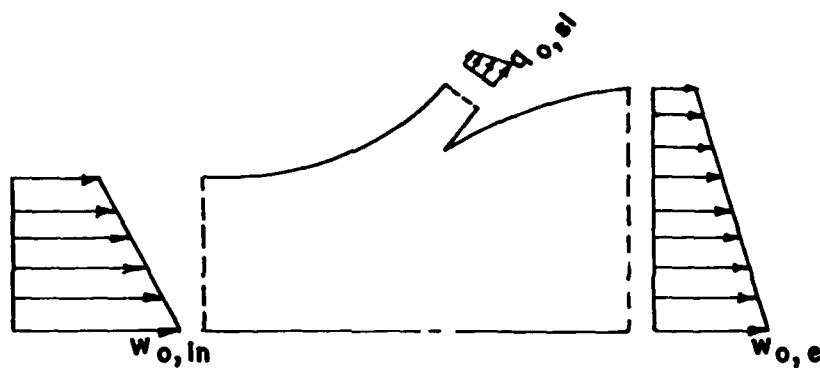


Figure 3. Velocity Distributions for Shear Flow

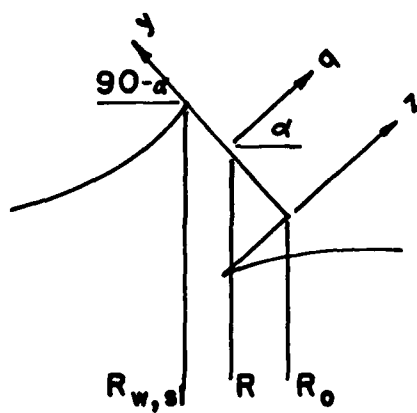


Figure 4. Coordinate System at Slot Exit

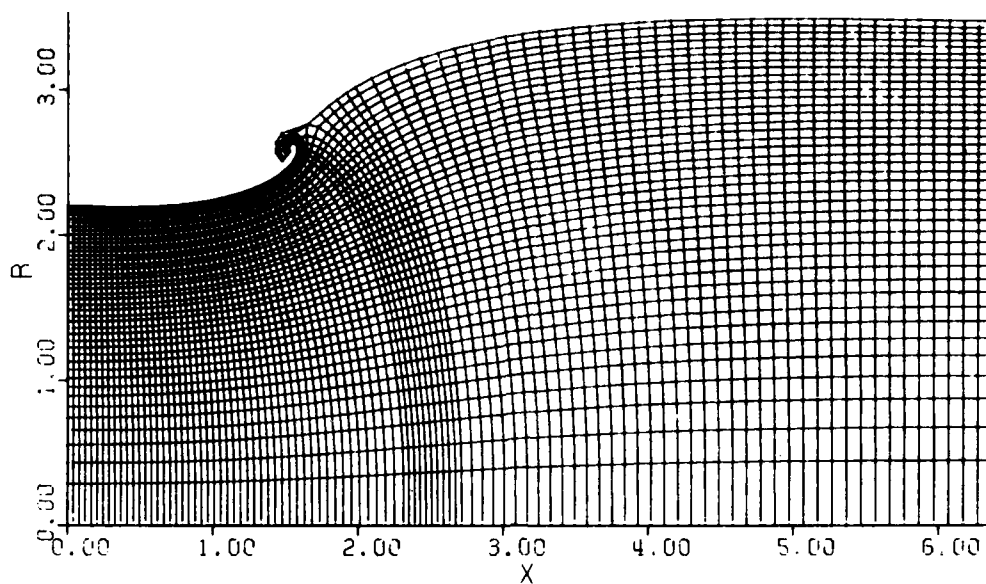


Figure 5. Computer Plot of  $\phi - \Psi$  Grid for an Axisymmetric Diffuser,  $AR = 2.5$ , Suction Rate = 5.6%

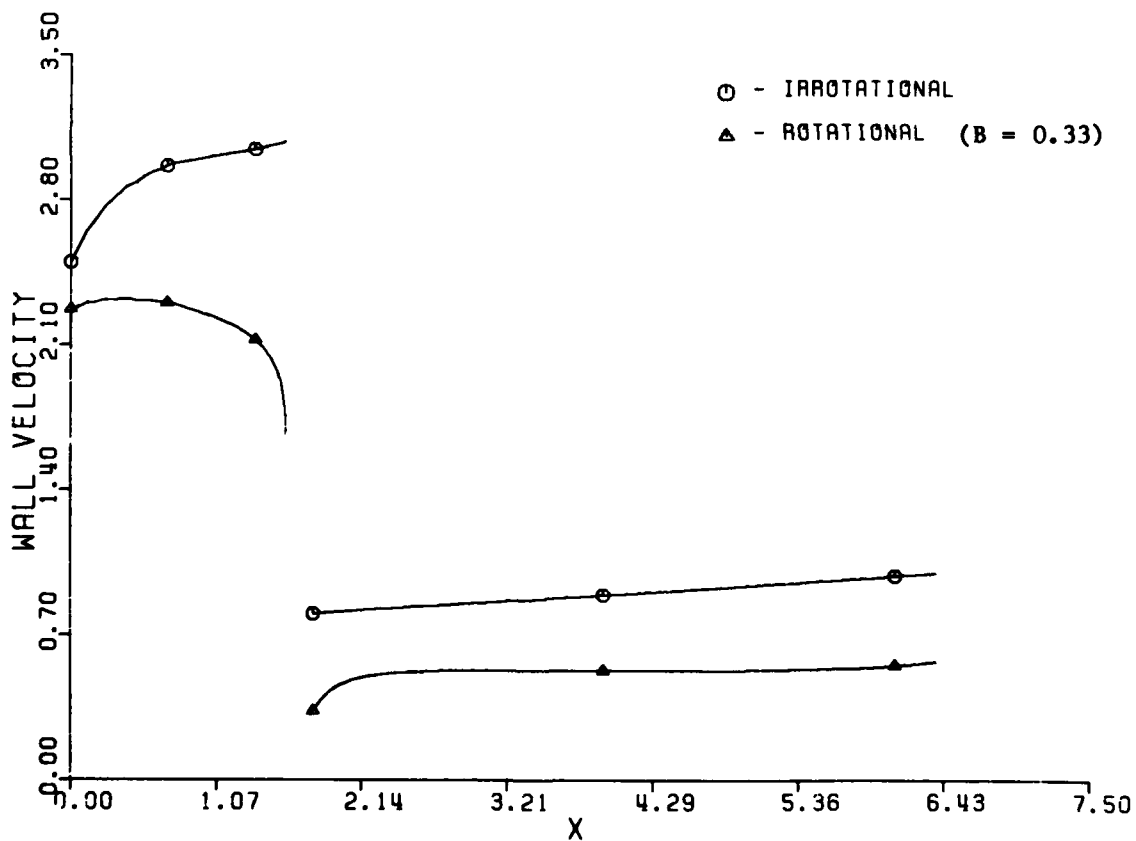


Figure 6. Velocity Distributions for Rotational and Irrotational Flow

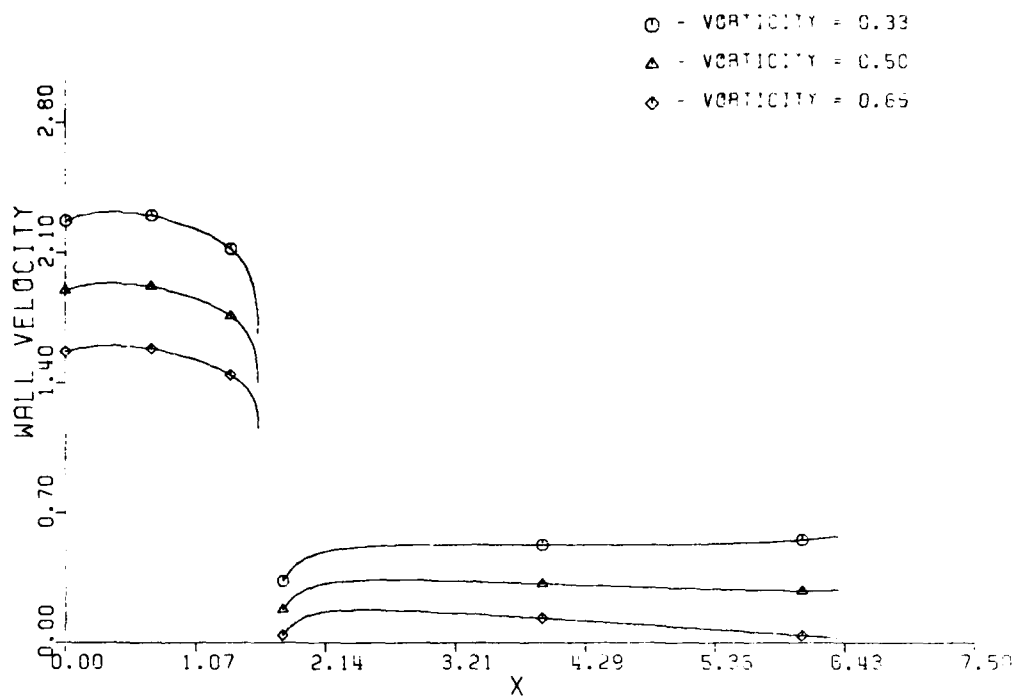


Figure 7. Velocity Distributions for Three Rotational Flows with Suction Rate of 5.6%

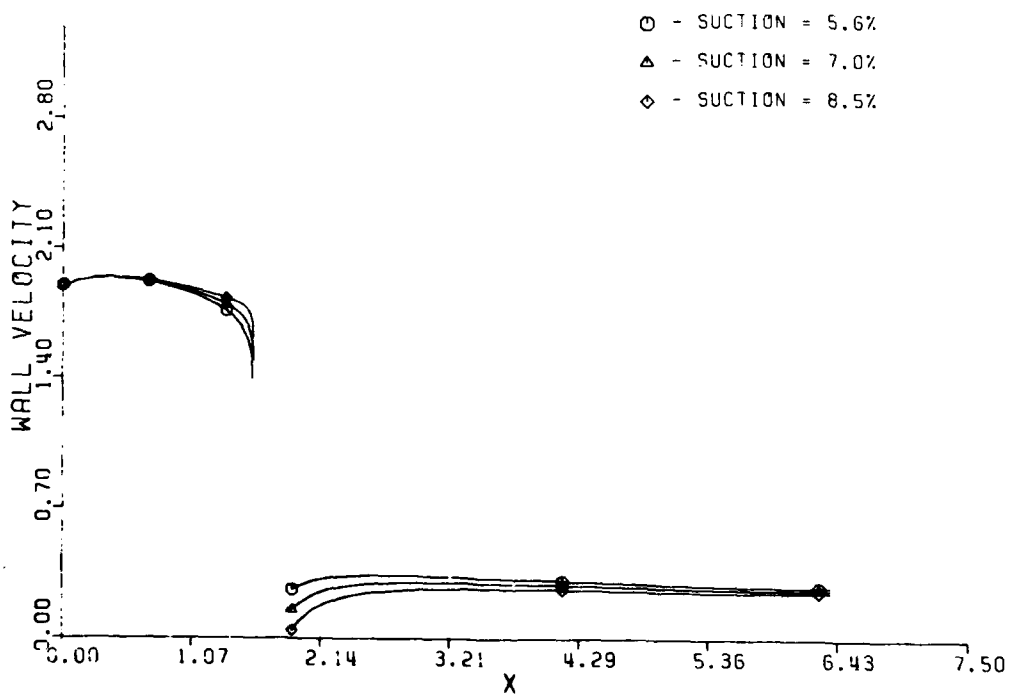


Figure 8. Velocity Distributions for Rotational Flow with  $B = 0.5$  and Three Suction Rates

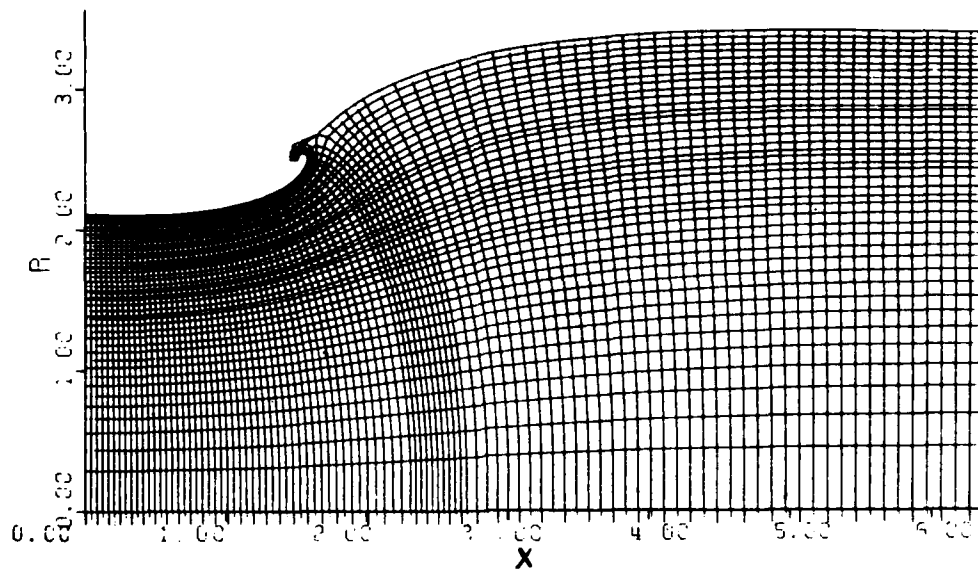


Figure 9. Computer Plot of  $\phi$ - $\psi$  Grid for an Axisymmetric Diffuser,  $AR = 2.5$ , Suction Rate = 5.6% (Change in Suction Slot)

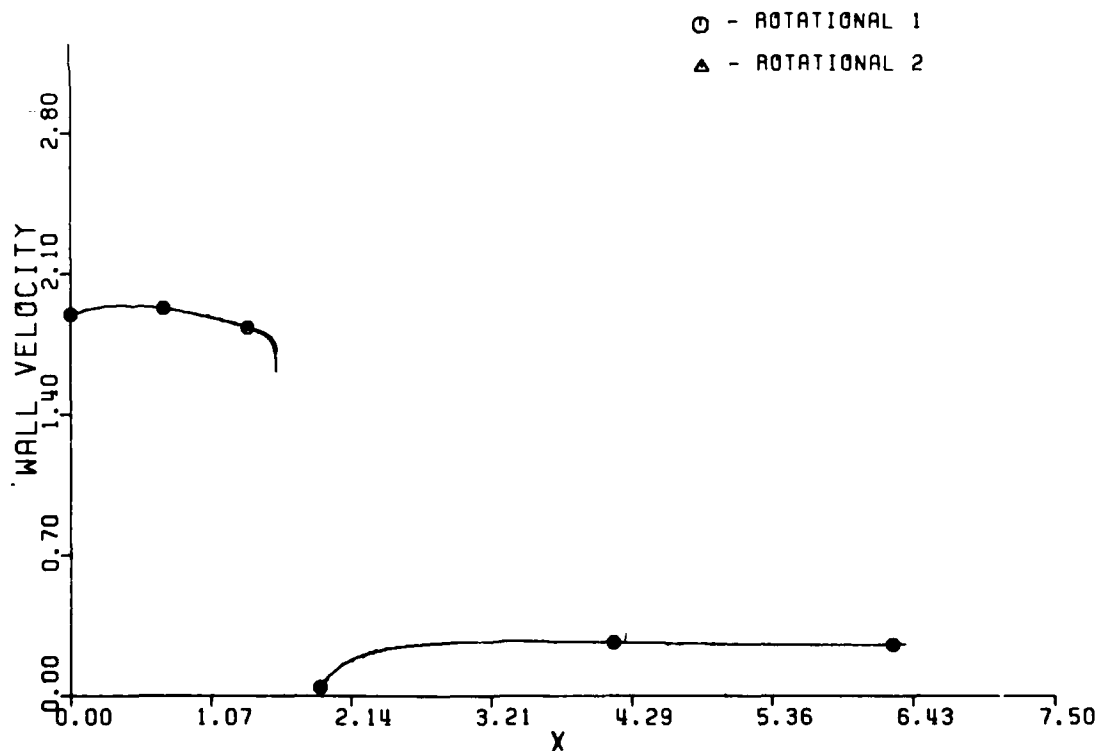


Figure 10. Velocity Distributions for Diffusers Represented in Figures 5 and 9 ( $B = 0.5$ , Suction Rate = 8.5%)

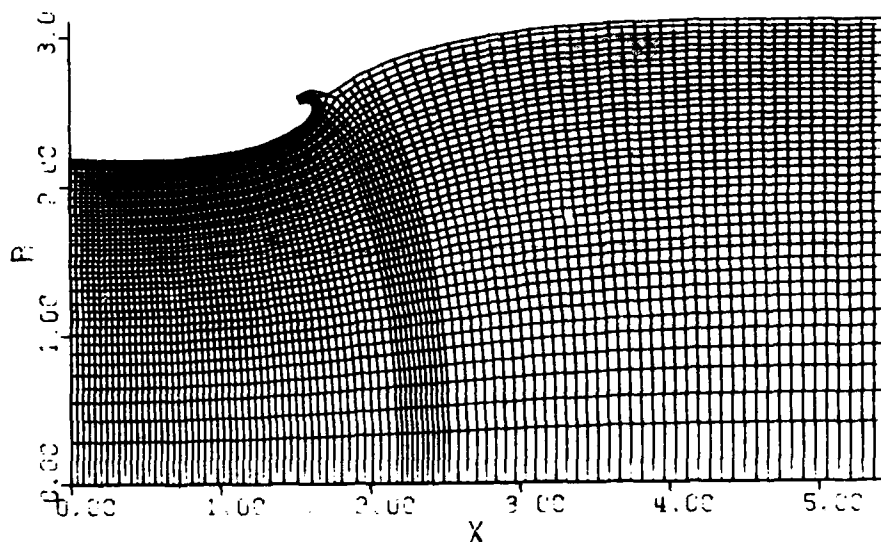


Figure 11. Computer Plot of  $\phi$ - $\psi$  Grid for an Axisymmetric Diffuser, AR = 2.0, Suction Rate = 5.6%

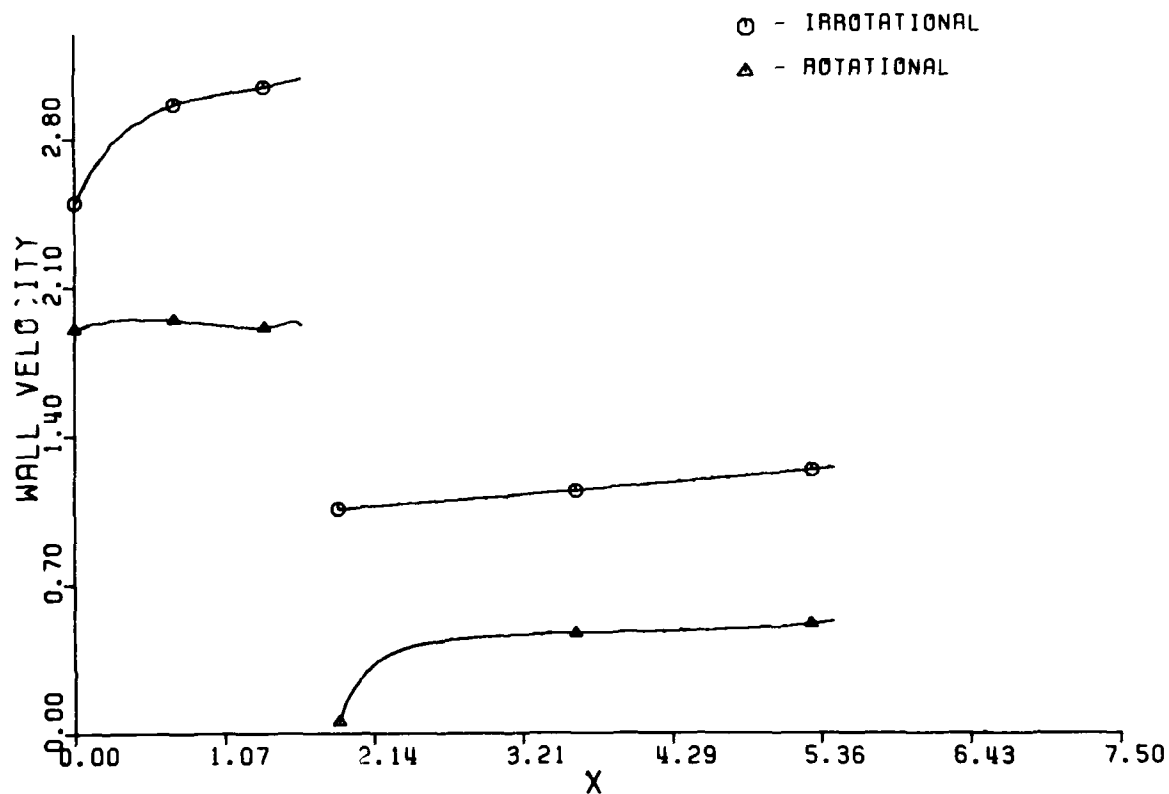


Figure 12. Velocity Distributions for Rotational and Irrotational Flows, B = 0.5, Suction Rate = 8.5%

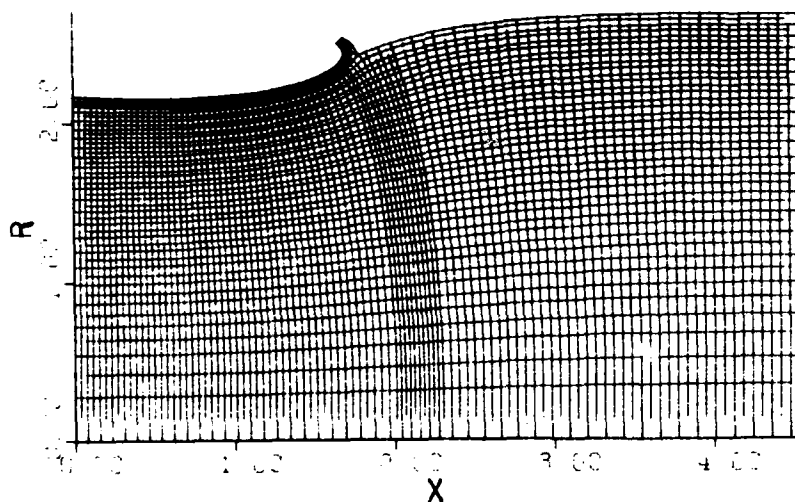


Figure 13. Computer Plot of  $\phi$ - $\psi$  Grid for an Axisymmetric Diffuser,  $AR = 1.5$ , Suction Rate = 8.5%

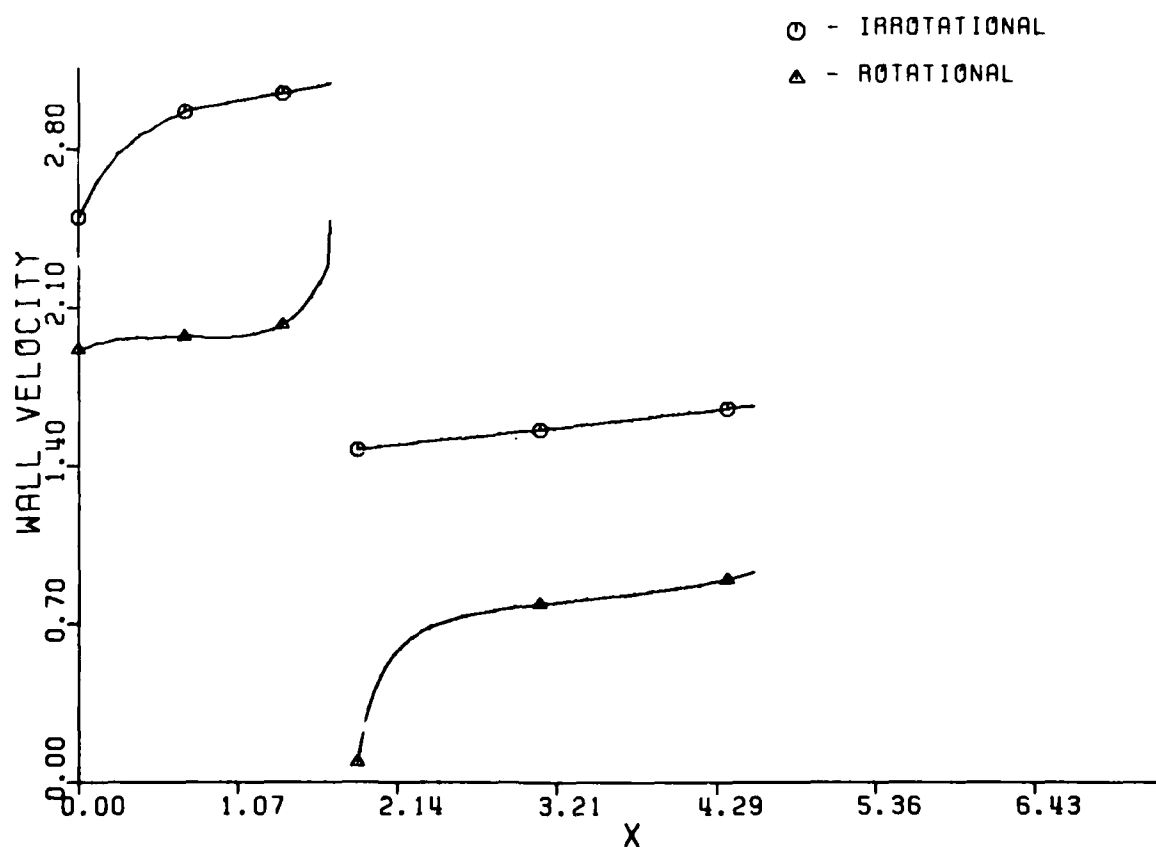
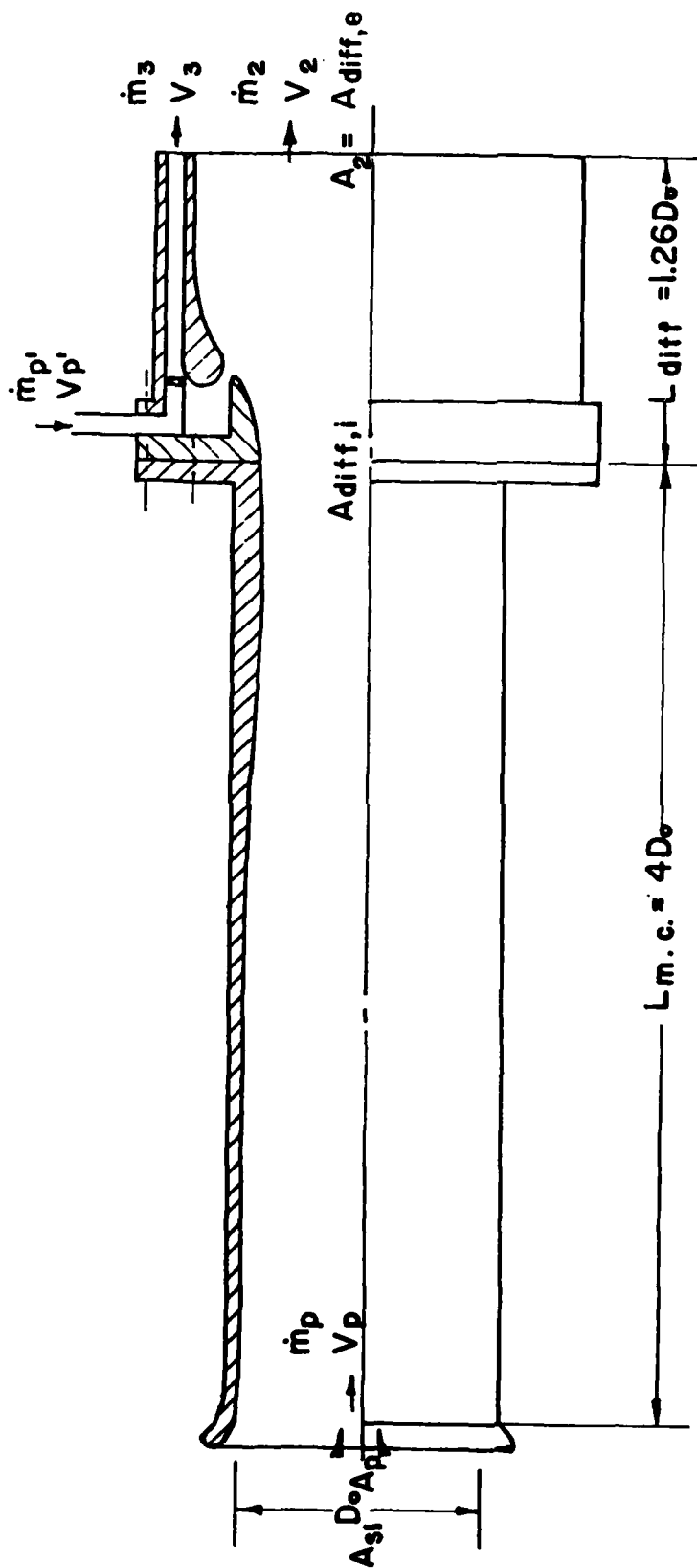


Figure 14. Velocity Distributions for Rotational and Irrational Flows,  $B = 0.5$ , Suction Rate = 8.5%





$$\frac{A_2}{A_{si}} = AR = 2 \quad \frac{A_{diff,e}}{A_{diff,i}} = AR_2 = 2.2 \quad \phi_2 = \frac{\dot{m}_2 V_2 + \dot{m}_3 V_3}{\dot{m}_p V_p + \dot{m}_{p'} V_{p'}} = 1.83$$

Figure 15. A Sample Air-to-Air Ejector with 10% Contraction for Mixing Chamber, No Deceleration Along Diffuser Wall

